Journal of Imaging Science and Technology® 53(5): 050501–050501-8, 2009.

Color Correction for Multiple Light Sources Using Profile Correction System

Vivek Maik and Joonki Paik
Image Processing and Intelligent Systems Laboratory, Graduate School of Advanced Imaging Science, Multimedia, and Film, Chung-Ang University, Seoul 156-756, Korea
E-mail: vivek5681@wm.cau.ac.kr

Dohee Cho and Dongwhan Har
Digital Scientific Imaging Laboratory, Graduate School of Advanced Imaging Science, Multimedia, and Film, Chung-Ang University, Seoul 156-756, Korea

Abstract. *In this article the authors propose a color correction system for images illuminated by multiple light sources. The proposed system can generate an illumination-invariant image under various light sources. Such illumination-invariant image acquisition becomes possible by adopting a user-defined profile connection space (UD-PCS) that generates custom profiles, which can be used to eliminate the effect of directional light sources. The proposed algorithm consists of the following steps: (i) input image capture with minimum of two light sources and reference Qpcard, (ii) estimation of color correction matrix and tone reproductive curves, (iii) modifying International Color Consortium profile tags to generate UD-PCS, and (iv) color mixture map extraction for fusion of input source images. Experiments were carried out on several test images with different light sources in order to prove the utility of the proposed algorithm.*

[DOI: 10.2352/J.ImagingSci.Technol.2009.53.5.050501]

INTRODUCTION

In the digital world, color is a significant attribute that helps us to define, understand, and identify objects. Color is an event that occurs with the combined presence of a light source, an object, and an observer. Any change in one of the three sources could result in a different color event. With day-to-day increase in digital products and more inventions appearing in the marketplace there is always a need to make sure that colors in these devices are standardized for easy handling, sharing, and broadcasting. This is one of the main objectives of the color management system (CMS). The CMS as shown in Figure 1 makes it possible to share a common image perception among various digital devices. Without proper color management a given image may appear differently depending on the imaging device. In summary, the role of the CMS is twofold: (i) it attaches a specific meaning of a color to images to make them unambiguous, and (ii) it allows each imaging device to produce the same color. To this end the International Color Consortium (ICC) has come up with a standard ICC-based CMS that has been used to produce visual matching across various digital devices. All ICC-based color management consists of three main components:

(1) Profile connection space (PCS) assigns color-specific, device-independent numerical values.
(2) Profiles relate the PCS color value with the device color format. This is a very important part of the entire color management process because the relationship provided by the profile makes the interdevice color conversion possible.
(3) The color management module (CMM) performs all the necessary calculations using the PCS values and the profile relationship with output device-dependent color values.

Figure 2 shows a block diagram of the proposed color correction algorithm. At the first stage we capture an input image that is illuminated by two or more light sources. After inspecting the image, an approximate direction of the light source is predicted, and this direction is used to capture a set of images at various angles with a Qpcard™ embedded in the image. (The Qpcard 201 is a color reference card. Some of the colors are mixed to resemble the spectral response of colors in real life, e.g., skin, sky, and forest; seven neutral patches, all of which have an almost straight spectral response, are included.)[1] Using the Qpcard colors from light source images A, B, and A and B, we were able to obtain the tone reproduction curve (TRC) and color correction matrix. These estimated correction parameters are later incorporated in to ICC profile to generate UD-PCS. After color correction with UD-PCS we generate color mixture map that will enable us to fuse all input images (A, B, A and B) to produce a single color corrected output. Detailed analysis of each of the modules in the block diagram is provided in the following sections of this paper.

RELATED WORKS

The color constancy problem has been a popular research topic in both human and computer vision areas. Most color constancy preserving algorithms have been based on restric-

Received Jul. 11, 2008; accepted for publication Mar. 20, 2009; published online Aug. 11, 2009.
1062-3701/2009/53(5)/050501/8/$20.00.

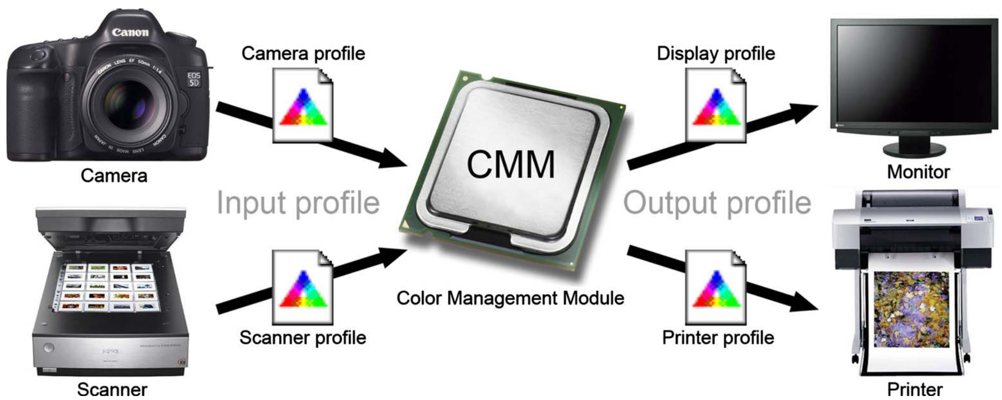

Figure 1. Color management system in the modern digital world.

tive assumptions including constant illumination.[2–4] This condition is not always satisfied especially when an object is illuminated by both a light bulb and daylight. To cope with this problem various constraints, such as the direction of an illumination source, measure of color temperature, and surface constraints, have been incorporated.[5–7]

The Retinex algorithm partially addresses the issue of varying illumination.[8,9] Retinex tries to eliminate variation in illumination and computes surface brightness for each of the three color channels independently. Retinex also assumes that within a single color channel small changes indicate intensity variation, while large changes indicate color variation. Therefore the smaller changes within a color channel can be reduced and larger changes can be reconstructed by summation. Unfortunately this method produces an error in classifying the intensity changes, which could result in serious mismatch in the recovered result.

Other color constancy methods exploit algebraic information in the image, statistical knowledge about light and color, geometric models of the color space, etc.[10–15] By representing surfaces and light sources in the form of linear combinations of finite-dimensional basis functions, the color constancy solution can be obtained.[10,11] Also the color constancy problem has been posed in a probabilistic framework, and a Bayesian approach is used to solve the problem.[12,13] The neural network approach[14] and the correlation framework[15] tend to clearly pinpoint the uncertainty of the problem. Image editors, such as ADOBE PHOTOSHOP,[16] have offered selection tools to segment regions lit by a single type of light.

Color constancy by gamut mapping has become popular since the research of Forsyth.[17] He developed an algorithm that solves for color constancy in two stages. The set of all possible illuminants is first recovered. From the recovered feasible set, a single illuminant is then chosen as an estimate of the unknown scene illuminant. Heuristic approaches replaced Forsyth's method using the mean-median process.[18,19] The method proposed in this article uses color profiles[20,21] from images with different illuminant sources and generate color corrected image. More specifically the proposed method computes the proportion of various pixels using reference white point and colors instead of choosing a proper illuminant map.

The major contributions of the proposed method include the following:

(i) It can estimate light mixture per pixel;
(ii) It can independently control light colors and intensities;
(iii) It can identify the light sources using the color profiles;

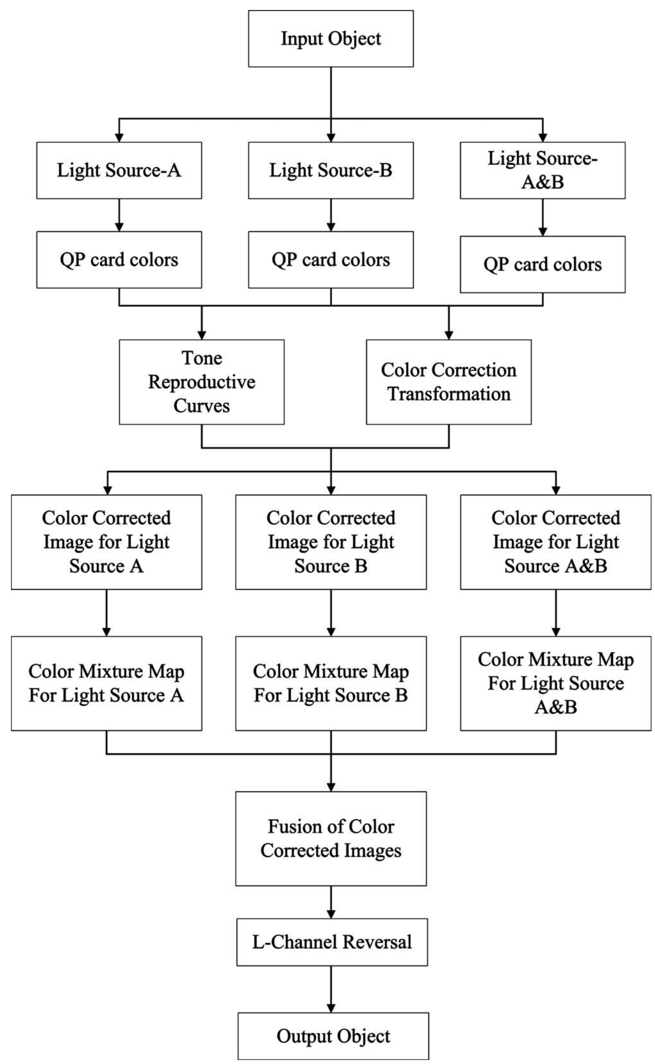

Figure 2. Block diagram of the proposed algorithm.

Table I. Technical terminologies for different images and profiles.

Notation	Meaning
Tungsten (*T*) image	Image obtained using tungsten light source
Fluorescent (*F*) image	Image obtained using fluorescent light source
Pseudo (*P*) image	Image obtained using mixed tungsten and fluorescent light sources.
T, *F*, and *P* profiles	Tungsten, fluorescent, and pseudocolor profiles respectively
T and *F* sources	Tungsten and fluorescent light source respectively
P source	Mixed tungsten and fluorescent light sources
T- and *F*-stop	Exposure setting for tungsten and fluorescent light sources, respectively

(iv) It does not increase the computational load compared with existing methods; and
(v) It does not require technical information on image processing.

IMAGE CAPTURE AND ESTIMATION OF COLOR CORRECTION PARAMETERS

In this section we will explain the process used to capture image and method by which the color correction parameters were estimated. For simplicity we base our whole explanation with reference to tungsten (*T*) and fluorescent (*F*) light sources. But the same algorithm can be extended to any light source in practice. Technical terminologies for different images and profiles are summarized in Table I.

Image Capture

Given our *T* and *F* light sources, we need to generate a set of *T*, *F*, and *P* images. In order to do that we propose the following experimental set up. We first capture images with different light sources using the Qpcard[1] color placed accurately in the direction of the incoming light source as shown in Figures 3 and 4. By doing so we can estimate the difference in colors caused by each of the light sources separately which can be later used in rectifying it. The Qpcard was

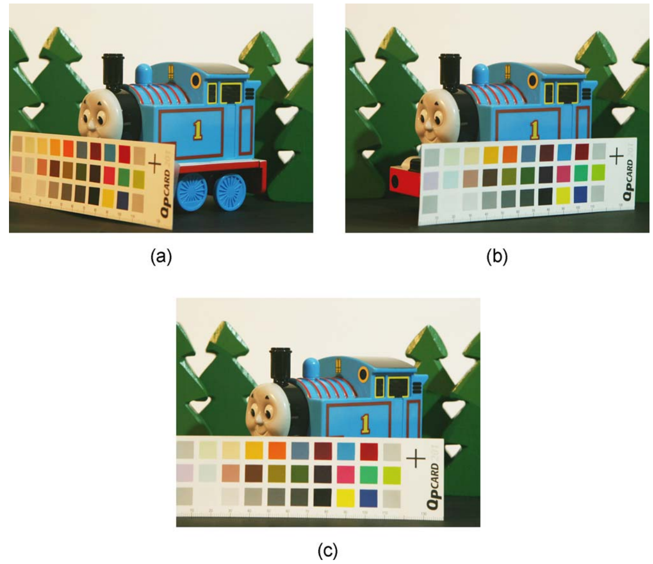

Figure 4. UD-PCS process: (a)–(c) represents the *T*, *F*, and *P* images with profile targets placed in the direction of the light source.

placed to face at an angle to each of *T* and *F* light sources. In case of *P* light source, the Qpcard was placed at the camera in the right angle direction to the object. In case of using *T* and *F* light sources the angular shift of the camera can be compensated by adjusting the exposure. For the *T* image shown in Fig. 4(a) the *T*-stop was −0.3, and for the *F* image shown in Fig. 4(b) the *F*-stop was −0.5. With such settings we ensure that the color gamut rendering is properly addressed. If the exposure setting is not adjusted with respect to camera's angular position, many out-of-gamut colors in the ICC profile can be produced, and these missing color values have to be rendered or replaced with different values. After acquiring images at desired exposure settings from *T*, *F*, and *P* light sources, we can correct the pixel colors using color transformation matrix and channel curve fitting explained in the following subsection.

Color Correction Parameters

Once we have captured the image, we extract the Qpcard from three different images (*T*, *F*, and *P*) and compare it

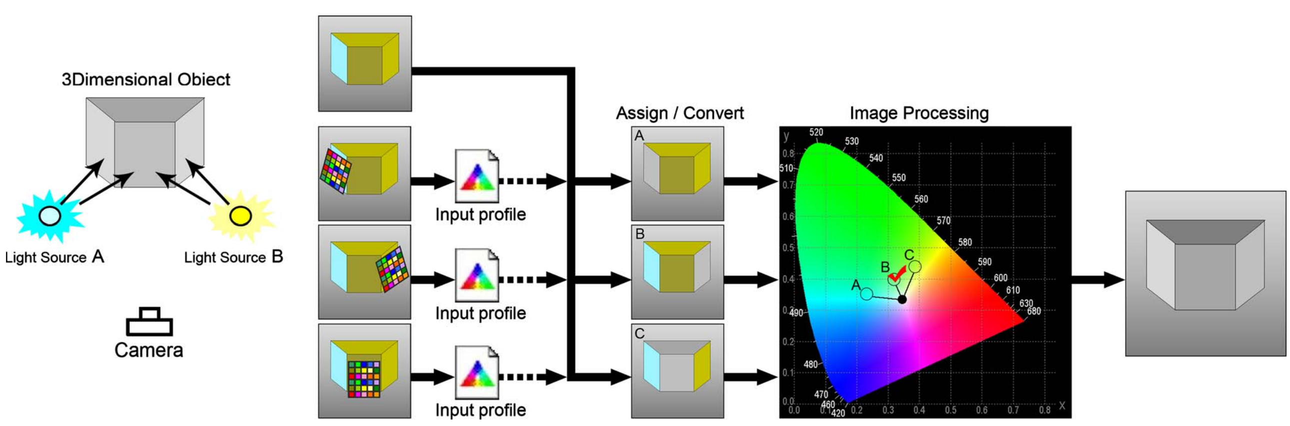

Figure 3. Block diagram of the proposed color constancy algorithm, which illustrates step-by-step functional flow from left to right.

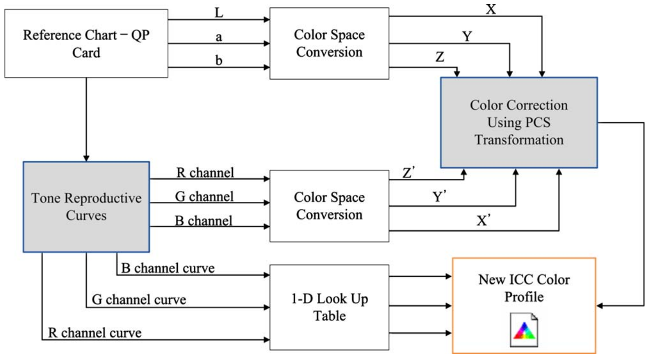

Figure 5. Schematic illustration of the TRC and color correction process for *T*, *F*, and *P* light sources.

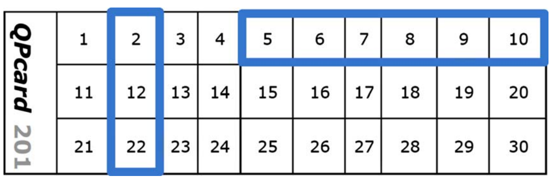

Figure 6. Qpcard patches. Patches 2, 12 and 22 represent the reference R, G and B colors, and patches 5–10 represent the reference gray levels for TRCs.

with a reference Qpcard to get color correction parameters. Figure 5 shows the block diagram of the color correction algorithm used in this paper. Tone reproductive curves (TRC) and pixel colors need to be adjusted in order to obtain the color corrected image. For the estimation of TRC, six patches located in the Qpcard as shown in Figure 6 are used. For each of the Qpcard in *T*, *F*, and *P* images, a function to fit the R, G, and B color values with the reference Qpcard is estimated using curve regression;

$$g(x) = a_1 f_1(x) + a_2 f_2(x) + a_3 f_3(x) + a_4 f_4(x), 0 \le x \le 1, \quad (1)$$

$$f_1(x) = 1, f_2(x) = x, f_3(x) = \sin(x), f_4(x) = \exp(x), \quad (2)$$

where a_n is an undetermined coefficient and x is the normalized color of the patch. The coefficients in Eq. (2) can be estimated by minimizing the least-squares difference between the color values of the selected patches in the *T*, *F*, and *P* images, and Qpcard. The color correction matrix is obtained by linear transformation which maps the colors of the Qpcard in *T*, *F*, and *P* images to those of the reference Qpcard colors. The transformation is estimated as follows:

$$M_{XYZ} = M_{Crr} M'_{XYZ}, \quad (3)$$

$$M_{XYZ} = \begin{bmatrix} X_1 & X_2 & & X_N \\ Y_1 & Y_2 & \dots & Y_N \\ Z_1 & Z_2 & & Z_N \end{bmatrix}, \quad (4)$$

$$M_{Crr} = \begin{bmatrix} m_{11} & m_{12} & m_{13} \\ m_{21} & m_{22} & m_{23} \\ m_{31} & m_{32} & m_{33} \end{bmatrix}, \quad (5)$$

$$M'_{XYZ} = \begin{bmatrix} X'_1 & X'_2 & & X'_N \\ Y'_1 & Y'_2 & \dots & Y'_N \\ Z'_1 & Z'_2 & & Z'_N \end{bmatrix}, \quad (6)$$

where X_i, Y_i, and Z_i denote the colors of the reference chart, and X'_i, Y'_i, and Z'_i are those of the color patches in the chart image. M_{Crr} is the color transformation matrix which maps the color of the image into those of the reference colors. By simple rearrangement using singular value decomposition (SVD), we can rewrite Eq. (3) as follows:

$$\begin{bmatrix} \mathrm{X}_1 \\ \mathrm{X}_2 \\ \vdots \\ \mathrm{X}_n \end{bmatrix} = \begin{bmatrix} \mathrm{X}'_1 & \mathrm{Y}'_1 & \mathrm{Z}'_1 \\ \mathrm{X}'_2 & \mathrm{Y}'_2 & \mathrm{Z}'_2 \\ & \vdots & \\ \mathrm{X}'_N & \mathrm{Y}'_N & \mathrm{Z}'_n \end{bmatrix} \begin{bmatrix} \mathrm{m}_{11} \\ \mathrm{m}_{12} \\ \mathrm{m}_{13} \end{bmatrix}, \quad (7)$$

$$\begin{bmatrix} Y_1 \\ Y_2 \\ \vdots \\ Y_n \end{bmatrix} = \begin{bmatrix} X'_1 & Y'_1 & Z'_1 \\ X'_2 & Y'_2 & Z'_2 \\ & \vdots & \\ X'_N & Y'_N & Z'_n \end{bmatrix} \begin{bmatrix} m_{21} \\ m_{22} \\ m_{23} \end{bmatrix}, \quad (8)$$

$$\begin{bmatrix} Z_1 \\ Z_2 \\ \vdots \\ Z_n \end{bmatrix} = \left[\begin{bmatrix} X'_1 & Y'_1 & Z'_1 \\ X'_2 & Y'_2 & Z'_2 \\ & \vdots & \\ X'_N & Y'_N & Z'_n \end{bmatrix}\right] \begin{bmatrix} m_{31} \\ m_{32} \\ m_{33} \end{bmatrix}. \quad (9)$$

UD-PCS GENERATION AND COLOR MIXTURE MODEL

UD-PCS Generation

In order to be able to recreate the proposed algorithm, the vital challenge would be to create a UD-PCS which can be used as a standard for the *P* light source images. Estimated color correction matrix values can be embedded in the ICC (Ref. 22) profile. These values are incorporated into the profile tags according to the specification of ICC. 1:2004-10: mediaWhitePointTag is set to the white point adjustment of the D65 light source. The redMatrixColumnTag, greenMatrixColumnTag, and blueMatrixColumnTag are originally intended to transform the device color space to PCS. The proposed system, however, applies the color correction matrix M_{Crr} in each of the three color tags as follows:

$$M_{Crr} = \begin{bmatrix} m_{11} & m_{12} & m_{13} \\ m_{21} & m_{22} & m_{23} \\ m_{31} & m_{32} & m_{33} \end{bmatrix} \quad (10)$$

$$= \begin{bmatrix} \text{redMatrixColumn}_x & \text{greenMatrixColumn}_x & \text{blueMatrixColumn}_x \\ \text{redMatrixColumn}_y & \text{greenMatrixColumn}_y & \text{blueMatrixColumn}_y \\ \text{redMatrixColumn}_z & \text{greenMatrixColumn}_z & \text{blueMatrixColumn}_z \end{bmatrix}. \quad (11)$$

When applying the color correction matrix it is important to take into consideration the chromatic adaptation transformation, since the illuminant of the color device is not equal to the PCS. ICC. 1:2004-10 recommends the linear Bradford model for the chromatic adaptive transformation which is given by M_{CAF};

$$M_{CAF} = \begin{bmatrix} t_{11} & t_{12} & t_{13} \\ t_{21} & t_{22} & t_{23} \\ t_{31} & t_{32} & t_{33} \end{bmatrix} = \begin{bmatrix} 0.436052 & 0.385082 & 0.143087 \\ 0.222492 & 0.716886 & 0.060621 \\ 0.013929 & 0.097097 & 0.714185 \end{bmatrix}, \quad (12)$$

$$M_{Crr}^{CAF} = M_{Crr} M_{CAF}, \quad (13)$$

where M_{Crr}^{CAF} represents the color correction matrix after chromatic adaptive transformation. Tone reproductive control tags: the TRC's for each of the three color channels are preserved in each of rTRCTag, gTRCTag, and bTRCTag. The estimated R, G, and B channel curves are used to map the input color pixels to output color pixels using a one-dimensional look-up table (LUT) as follows:

$$\text{redTRC}[i] = g_R(x_i), \quad (14)$$

$$\text{greenTRC}[i] = g_G(x_i), \quad (15)$$

$$\text{blueTRC}[i] = g_B(x_i), \quad (16)$$

where i represents the number of color pixels. Figure 7 gives schematic representation of the above algorithm and Table II represents the ICC profile tag structure.

Color Mixture Model

The UD-PCS which makes use of modified profiles with color correction information can be applied to T, F, and P source images to obtain corresponding color corrected images. In order to obtain the final color enhanced image the proposed algorithms uses a color mixture model to fuse these three color corrected images (Figures 8 and 9). The color mixture map can be obtained by measuring the distance of the white point in the T, F, and P source images compared with the reference chart white color as shown in Fig. 3. This color difference (delta E) enable us to estimate the proportion of color in each of T, F, and P images required to produce the final fused color enhanced image;

$$dE_T = Wp_R - Wp_T, \quad (17)$$

$$dE_F = Wp_R - Wp_F, \quad (18)$$

$$dE_P = Wp_R - Wp_P, \quad (19)$$

where (dE_T, dE_F, dE_P) and (Wp_T, Wp_F, Wp_P) represent the ΔE color difference for T, F, and P images, and Wp represents the reference white point. Finally the color mixture proportion can be obtained as

Table II. ICC profile tags.

Tag	Signature	Data type
mediaWhitePointTag	wtpt	XYZType
mediaBlackPointTag	bkpt	XYZType
CopyrightTag	cprt	multiLocalizedUnicodeTag
profileDescriptionTag	desc	multiLocalizedUnicodeTag
redMatrixColumnTag	rXYZ	XYZType
greenMatrixColumnTag	gXYZ	XYZType
blueMatrixColumnTag	bXYZ	XYZType
redTRCTag	rTRC	curveType
greenTRCTag	gTRC	curveType
blueTRCTag	bTRC	curveType

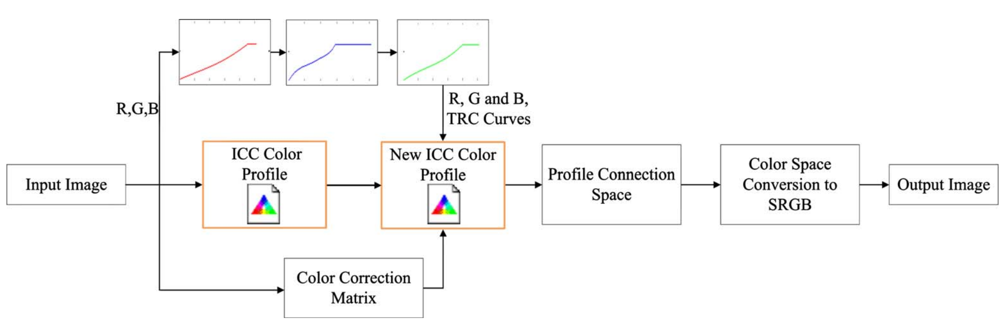

Figure 7. Generation of color corrected output image using UD-PCS.

$$I_{out} = \frac{T^{corr}}{dE_T/dE_T + dE_F + dE_P} + \frac{F^{corr}}{dE_T/dE_T + dE_F + dE_P} + \frac{P^{corr}}{dE_T/dE_T + dE_F + dE_P}, \quad (20)$$

where $(T^{Corr}, T^{Corr}, P^{Corr})$ represent the color corrected images for T, F, and P light sources and I_{out}^{Corr} represent the final fused image. For the ideal case where each source image contributes equally we have that

$$\frac{dE_{TorForP}}{(dE_T + dE_F + dE_P)} = 0.33. \quad (21)$$

L-Channel Reversal

The color mixture process among various channels may result in significant errors including block artifacts and color mismatching. Block artifacts are most commonly the result of using a compression standard such as JPEG, whereas color mismatching usually occurs in transition edge boundaries as shown in Figure 10. Since most artifacts are highly related with pixel intensity than color values we replace the L channel with the original P image. The L-channel replacement can reduce color mixture artifact as shown in Fig. 10.

EXPERIMENTAL RESULTS

Experiments

The proposed algorithm has been tested on both studio and real scene images. In all cases the illumination source consists of tungsten light coming from one direction mixed with fluorescent light coming in the other direction along with daylight. For the qualitative evaluation of the results we have used a color scatter plot in the a-b color space as well as the color mixture map for image. Figures 11(a)–11(c) show images taken with T, F, and P light sources. Figures 11(d)–11(f) show color mixture maps from the corresponding images shown in Figs. 11(a)–11(c), respectively. We note that Fig. 11(d) has the highest error on the left side and Fig. 11(e) has the highest error on the right side. This indicates the illumination on either side of the images has been counterattacked by the color profile and the mixing process. Figure 11(g) shows the image finally obtained by the mixture of the three color channels using proportions from Figs. 11(d)–11(f). The color scatter plot of the final images is shown in Figures 12 and 13 for qualitative comparison. As shown in Fig. 12(a) the scatter plot is not uniformly distributed across the a-b color domain space thereby indicating lower color quality of the images. On the other hand as shown in Fig. 12(b), the proposed method tends to distribute the colors more uniformly for higher visual quality.

Finally we have presented additional qualitative visual comparison in regions of color gradients or transition. In these regions the original images with multiple illuminant sources produce scatter plots as shown in Fig. 13(a), where the color distribution is more evenly distributed, whereas the ideal case requires more compact distribution for proper visual quality. As shown in Figs. 13(b) and 13(c) the color distribution should be more spread out for the visual quality to be as good as that of the proposed method. Similar test results are shown for synthetic test images in Figure 14. The synthetic test images were generated using a Canon D-10 camera with light settings tuned to fluorescent and tungsten. With these settings we were able to generate images outside the white box and provide high quality images. Similar test results using the proposed algorithms were carried out on some natural indoor and outdoor images as shown in Figs. 14(a) and 14(b), respectively.

Performance Comparison

We have tested the proposed algorithm with different sets of light sources in addition to tungsten and fluorescent used in the original version. Light sources tested include Horizon (1750 Lux, 6319K), CWF (1606 Lux, 3970K), A (1969 Lux,

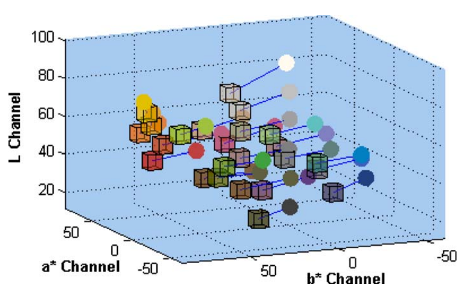

Figure 8. Color difference between Qpcard colors in T source image and reference chart. The color difference of white point location is used in computing the color mixture map which is used to fuse T, F, and P source images.

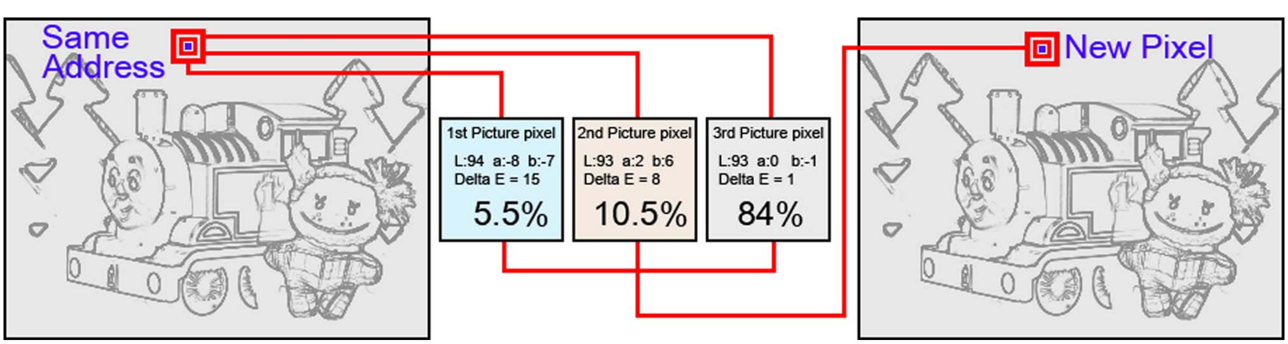

Figure 9. Pixel assignment process. The pixels from each pixel-corrected image are selected in appropriate proportions and merged to form the final image.

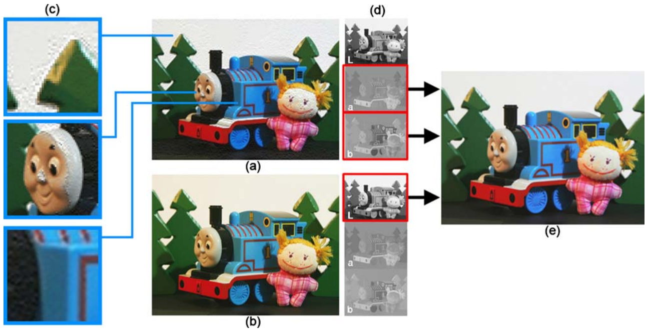

Figure 10. *L*-channel reversal process. (a) *P* image, (b) Fused final image, (c) parts of the image with color mixture artifacts, (d) LAB channels of the images (a) and (b), and (e) the *L*-channel replaced image.

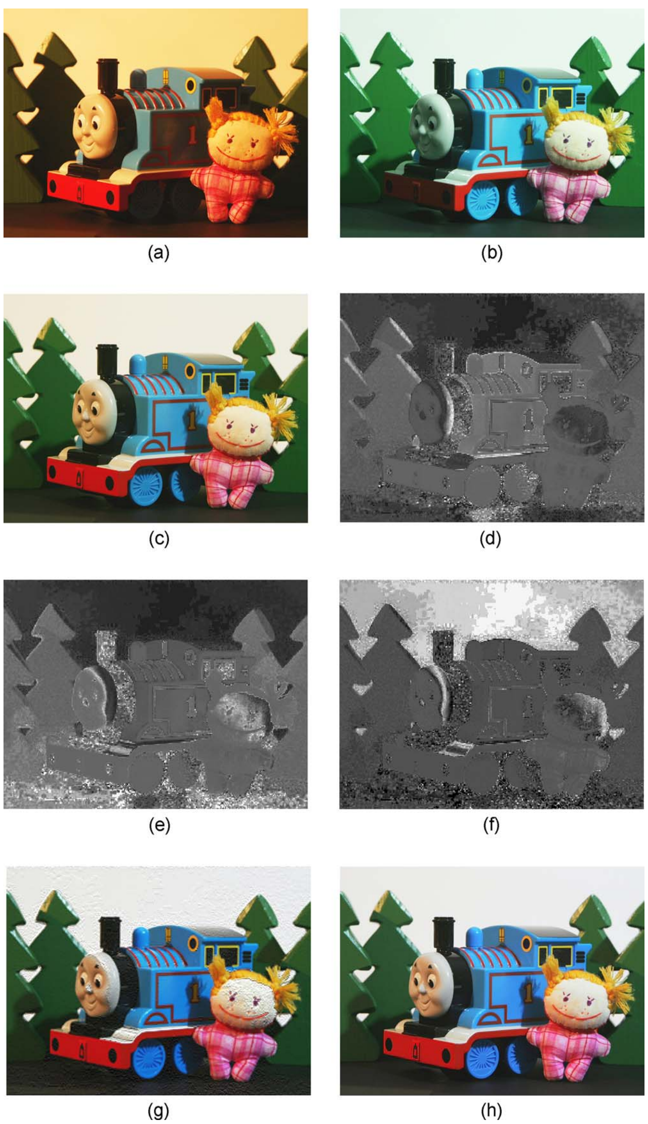

Figure 11. Experimental results: (a) *T* source image, (b) *F* source image, (c) *P* source image, (d)–(f) color mixture map of *T*, *F*, and *P* source images, and (g)–(h) final fused image before and after *L*-channel replacement.

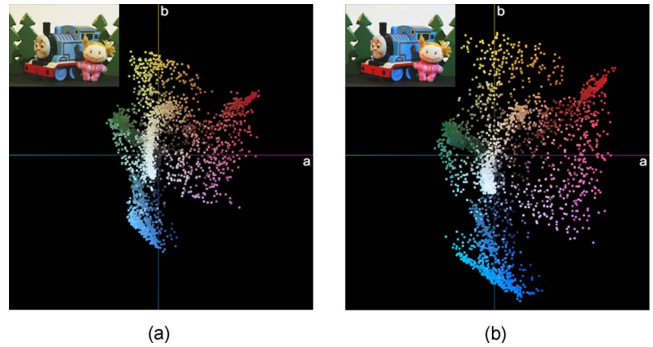

Figure 12. Color scatter plot. (a) *P* image, (b) *P* image after applying the proposed method. The colors are uniformly distributed over the color space.

2863K), U30 (1675 Lux, 2843K), and D-65 (1660 Lux, 6319K). Since one of the main contributions of our paper is to deal with generation of UD-PCS, we have compared the performance of our method with some standard off the shelf profiling tools which includes PROFILE MAKER™ and I-1 as shown in Table III.

CONCLUSIONS

In this article we have proposed a color constancy approach using the color profile correction method. The proposed method is easier to apply to images and does not require an excessive computational load. The color correction process

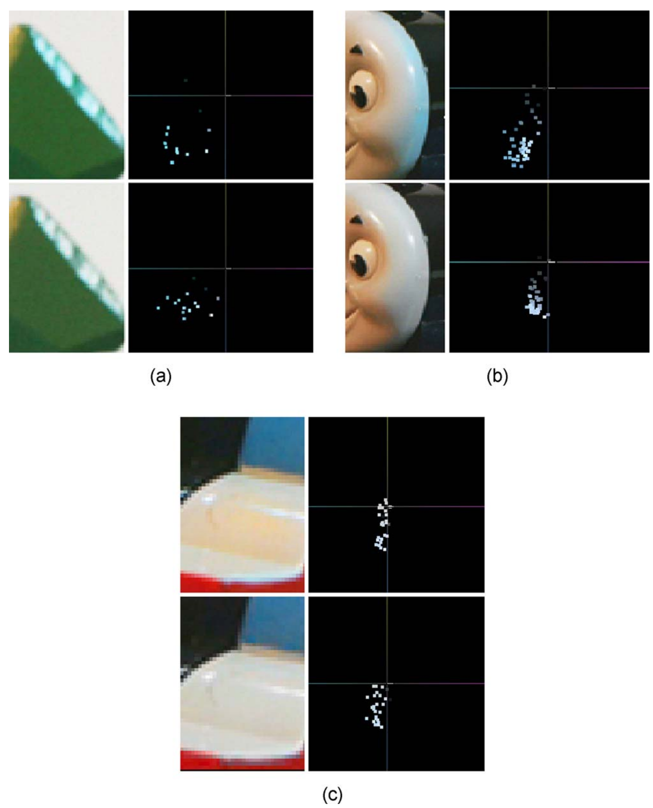

Figure 13. Color scatter plot at specific regions of the image. The "above" images in (a)-(c) represent the scatter plot of the original *P* image and "below" images show the difference after the color constancy algorithm have been applied.

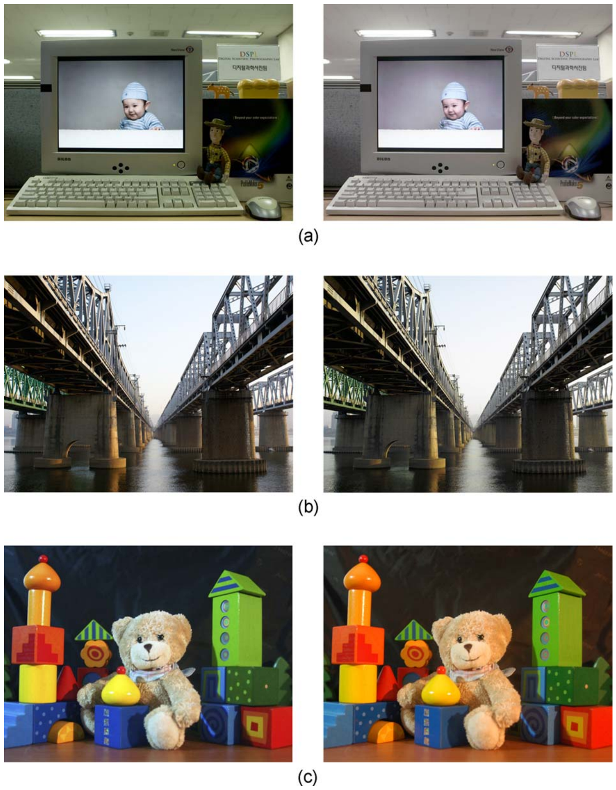

Figure 14. Experimental results on (a) indoor, (b) outdoor, and (c) synthetic images.

Table III. Root-mean-square error comparison of the proposed algorithm with standard profiling software.

Light Sources	PROFILE MAKER	I-1	Proposed method
A-CWF	119.4761	67.7193	53.0244
CWF-HORIZON	127.2063	81.3686	53.2583
CWF-U30	121.8296	69.035	59.539
D65-A	106.7238	39.8982	35.9207
D65-CWF	103.0539	35.5892	31.9188
D65-U30	108.719	45.3516	42.1452
HORIZON-A	122.0171	70.1249	41.2256
HORIZON-U30	154.8729	123.3306	52.9711
U30-A	130.1626	83.9268	53.8381

can be effectively adapted to UD-PCS to build an ICC color profile. The color mixture map further improves the accuracy of the algorithm. Future work will be focused on making quantitative comparison with existing relevant algorithms including gamut mapping, constraint-based, and computational methods to name a few. Another useful extension would be to include three-dimensional objects and to apply the proposed algorithm to them.

ACKNOWLEDGMENTS

This work was supported by National Research Foundation (NRF) grant by the Korea government (MEST) (2009-0081059), Seoul Future Contents Convergence (SFCC) Cluster established by Seoul R&BD program, Korean Ministry of Knowledge Economy under the Home Network Research Center (HNRC-ITRC), and the Industrial Technology Development program of the Ministry of Knowledge and Economy (MKE) of Korea.

REFERENCES

[1] L. Kjellberg, Qpcard Key to Color Version 201, www.qpcard.se, accessed from 2005.

[2] S. Shafer, "Using color to separate reflection components", Color Res. Appl. **21**, 1210 (1999).

[3] H. Lee, E. Breneman, and C. Schulte, "Modeling light reflection for computer color vision", IEEE Trans. Pattern Anal. Mach. Intell. **12**, 402 (1986).

[4] G. Buchsbaum, "A spatial processor model for object color perception", J. Franklin Inst. **310**, 1 (1980).

[5] J. Parkkinen, T. Jaaskelainen, and M. Kuittinen, "Spectral representation of color images", *Proc. IEEE Ninth International Conference Pattern Recognition* (IEEE, Piscataway, NJ, 1983) Vol. **2**, pp. 933–935.

[6] G. Finlayson and B. Funt, "Color constancy with shadows in perception: Special Issue", *17th European Conference Visual Perception* (Pion, London, 1985) Vol. **23**, pp. 89–90.

[7] M. D'Zmura, "Color constancy: surface color from changing illumination", J. Opt. Soc. Am. A Opt. Image Sci. Vis **9**, 490–493 (1992).

[8] K. Barnard, G. Finlayson, and B. Funt, "Color constancy for scenes with varying illumination", J. Comp. Vision and Image Understanding **65**, 311–321 (1997).

[9] B. K. P. Horn, ""Determining lightness from an image", Comput. Vis. Graph. Image Process. **3**, 277 (1974).

[10] P. Hubel, J. Holm, G. Finlayson, and M. Drew, "Matrix calculations for digital photography", *Proc. IS&T/SID Fifth Color Imaging Conference* (IS&T, Springfield, VA, 1997) pp. 105–111.

[11] M. D'Zmura and G. Iverson, "Color constancy: basic theory of two-stage linear recovery of spectral descriptions for lights and surfaces", J. Opt. Soc. Am. **10**, 2148 (1987).

[12] M. D'Zmura and G. Iverson, *Papers in Honor of Tarow Indow's 70th Birthday* (Laurence Erlbaum, Mahwah, NJ, 1994).

[13] D. Brainard and W. Freeman, "Bayesian color constancy", J. Opt. Soc. Am. **14**, 1393 (1997).

[14] B. Funt, V. Cardei, and K. Barnard, "Learning color constancy", *Proc. IS&T/SID Fourth Color Imaging Conference* (IS&T, Springfield, VA, 1996) pp. 58–60.

[15] G. Finlayson, P. Hubel, and S. Hordley, "Color by correlation", *Proc. IS&T/SID Fifth Color Imaging Conference* (IS&T, Springfield, VA, 1997) pp. 6–11.

[16] D. Marguis, *Photoshop LAB color* (Pearson Education, Peachpit Press, Berkeley, CA, 1997).

[17] D. Forsyth, "A novel algorithm for color constancy", Int. J. Comput. Vis. **5**, 5 (1990).

[18] G. Finlayson and S. Hordley, "Selection for gamut mapping color constancy", *Proc. 8th British Machine Vision Conference* (British Machine Vision Association, Essex, England, 1997) Vol. **2**, pp. 630–639.

[19] G. Finlayson, "Color in perspective", IEEE Trans. Pattern Anal. Mach. Intell. **18**, 1034 (1996).

[20] B. Fraser, C. Murphy, and F. Bunting, *Real World Color Management* (Pearson Education, Peachpit, Berkeley, CA, 2003).

[21] A. Sharma, *Understanding Color Management* (Thomson-Delmar Learning, New York, 2002).

[22] *ICC, 1: 2004–10 Imaging Technology Color Management, Architecture, Profile Format and Data Structure* (ICC, Reston, VA, 1997), www.color.org, ICC, ICC profile format specification.